# The effect of (Ti + Al): V ratio on the structure and oxidation behaviour of TiAlN/VN nano-scale multilayer coatings

LEWIS, D. B., CREASEY, S. J., ZHOU, Z., FORSYTH, J. J., EHIASARIAN, A. P. <http://orcid.org/0000-0001-6080-3946>, HOVSEPIAN, P. E. <http://orcid.org/0000-0002-1047-0407>, LUO, Q. <http://orcid.org/0000-0003-4102-2129>, RAINFORTH, W. M. and MUNZ, W. D.



**Published version**

LEWIS, D. B., CREASEY, S. J., ZHOU, Z., FORSYTH, J. J., EHIASARIAN, A. P., HOVSEPIAN, P. E., LUO, Q., RAINFORTH, W. M. and MUNZ, W. D. (2003). The effect of (Ti + Al): V ratio on the structure and oxidation behaviour of TiAlN/VN nano-scale multilayer coatings. Surface and coatings technology, 177, 252-259.

# The effect of (Ti+Al):V ratio on the structure and oxidation behaviour of TiAlN/VN nano-scale multilayer coatings

D.B. Lewis*, S. Creasey[a], Z. Zhou[b], J.J. Forsyth[a], A.P. Ehiasarian[a], P.Eh. Hovsepian[a], Q. Luo[a], W.M. Rainforth[b], W.-D. Munz[a]

[a] Materials Research Institute, Sheffield Hallam University, Sheffield S1 1WB, UK
[b] Department of Engineering Materials, University of Sheffield, Sheffield S1 3JD, UK

**Abstract:** Nano-scaled multilayered TiAlN/VN coatings have been grown on stainless steel and M2 high speed steel substrates at $U_B$ = -85 V in an industrial, four target, Hauzer HTC 1000 coater using combined cathodic steered arc etching/unbalanced magnetron sputtering. X-ray diffraction (XRD) has been used to investigate the effects of process parameters (Target Power) on texture evolution (using texture parameter T*), development of residual stress ($\sin^2 \psi$ method) and nano-scale multilayer period. The composition of the coating was determined using energy dispersive X-ray analysis. The thermal behaviour of the coatings in air was studied using thermo-gravimetric analysis, XRD and scanning electron microscopy. The bi-layer period varied between 2.8 and 3.1 nm and in all cases a {1 1 0} texture developed with a maximum value T* = 4.9. The residual stress varied between -5.2 and -7.4 GPa. The onset of rapid oxidation occurred between 62° and 645 °C depending on the (Ti+Al):V ratio. After oxidation in air at 550 °C AlVO4, TiO2 and V2O5 phases were identified by XRD with the AlVO4, TiO2 being the major phases. The formation of AlVO4 appears to disrupt the formation of Al2O3 which imparts oxidation resistance to TiAlN based coatings. Increasing the temperature to 600 and 640 °C led to a dramatic increase in the formation of V2O5 which was highly oriented (001) with a plate-like morphology. At 640 °C there was no evidence of the coating on XRD. Increasing the temperature to 670°C led to further formation of AlVO4 and a dramatic reduction in V2O5.

**Keywords:** Nano-scale multilayers; TiAlN/VN coatings; Oxidation; X-ray diffraction; Scanning electron microscopy

## 1. Introduction

TiAlN/CrN, TiAlN/VN and CrN/NbN nano-scaled multilayered coatings with typical periods l between 3 and 4 nm have been successfully produced economically under production conditions in industrially sized coating equipment [1]. TiAlN/CrN [2,3] exhibits excellent high temperature wear resistance and oxidation resistance, whereas CrN/NbN [4,5], has excellent anti-corrosion performance. Nano-scaled, multilayered TiAlN/VN coatings exhibit at room temperature, low coefficients of friction, μ = 0.4–0.5 and low sliding wear coefficients of $1.2=10^{-17}$ $m^3N^{-1}m^{-1}$which is two orders of magnitude lower compared to TiAlN/CrN (μ = 0.7 , K = $2.38x10^{-16}$ $m^3N^{-1}m^{-1}$) and CrN/NbN (μ = 0.69, K = $2.1x10^{-15}$ $m^3N^{-1}m^{-1}$) systems. The lowest value of the coefficient of friction is due to the formation of a vanadium oxide ($V_2O_5$), which acts as a $V_2O_5$ dry lubricant [1]. At temperatures above 640 °C the VN component in the multilayer is completely oxidised to $V_2O_5$ and at temperatures above 670 °C, the $V_2O_5$ starts to melt resulting in loss of coating integrity making them unsuitable in higher temperature applications. However, one important area where the low coefficient of friction can be utilised is in the coating of M2 HSS cutting tools which have a maximum operating temperature of typically approximately 550°C. The lower coefficient of friction of these coatings may, therefore be particularly beneficial in the high speed machining of softer materials, e.g. Al alloys, Inconel alloys, where friction between work piece material and tool is of particular importance. This paper summarises results on the effect of (Ti+Al):V ratio on the structure and oxidation behaviour of TiAlN/VN nano-scale multilayer coatings.

## 2. Experimental details

TiAlN/VN coatings investigated were deposited by reactive unbalanced magnetron sputtering in a Hauzer Techno Coating HTC 1000-4 using the arc bond sputter process [6]. In all the processes 2 x V targets (99.9%) and 2 x Ti:Al (50:50) targets were used and the power applied to each target is given in Table 1. The coatings were deposited at bias voltages of $U_B$ = -75 V for 1.5h and $U_B$ = -85 V for 1.5 h using the target powers shown in Table 1. All the coatings were deposited at a constant temperature of 450 °C on to stainless steel and M2 HSS substrates in a common Ar+N2 atmosphere at a total pressure of 4.5 x $10^{-3}$ mbar. A more detailed description of the process parameters used is described elsewhere [1,7–10].

The textures present in the as-deposited coatings were determined by the Harris inverse pole figure method (Texture T*) [11]. The bi-layer period of the nano-scale multilayer, D, was measured directly in the low angle region from the standard Bragg's equation [9]. Glancing angle parallel

**Table 1** Target configuration, analysis and bi-layer thickness

| Sample | Power to target (kW) | | | | Al (at.%) | Ti (at.%) | V (at.%) | (Ti+Al):V | Bi-layer thickness (nm) |
|---|---|---|---|---|---|---|---|---|---|
| | Ti–Al | Ti–Al | V | V | | | | | |
| 1 | 10 | 10 | 5.5 | 5.5 | 32.5 | 30.9 | 36.6 | 1.73 | 2.8 |
| 2 | 10 | 10 | 7 | 7 | 28.5 | 27.8 | 43.7 | 1.29 | 3.0 |
| 3 | 10 | 10 | 8 | 8 | 26.9 | 26.3 | 46.8 | 1.14 | 3.0 |
| 4 | 11.5 | 11.5 | 7 | 7 | 32.2 | 29.2 | 38.6 | 1.59 | 3.1 |

beam geometry was used to determine the state of residual stress present in the coatings [12]. The products which formed on the coatings surface after oxidation were identified by X-ray diffraction (XRD) using glancing angle (1° incidence) and $\theta/2\theta$ geometries. The morphology of the oxidized surfaces was investigated using a FEI environmental scanning electron microscope. The atomic percentage of the metallic elements in each coating was determined using a ZAF 4 corrected energy dispersive X-ray (EDX) analysis. A Cahn TG 121 microbalance was used for the thermo-gravimetry work. The hardness was measured using a Knoop indenter,$(HK)_{0.025}$. Pin-on-disc measurements were made in dry sliding wear conditions using $Al_2O_3$ balls, a 5 N load at a linear speed of 0.1 $ms^{-1}$.

## 3. Results and discussion

### *3.1. Coating characterisation*

#### *3.1.1. Composition*

Elemental analyses of the metallic elements in the coatings under investigation are shown in Table 1. A scan be predicted from the deposition parameters the (Ti+Al):V ratio decreases as the power to the pure V targets was increased, see Table 1.

#### *3.1.2. Structural analysis*

Low angle XRD was used to determine the bi-layer periods, D of the nano-scale multilayers, which were in the range of 2.8–3.1 nm, see Table 1. Texture measurements using the Harris inverse pole figure method for the four specimens under investigation are given in Table 2. In all cases the films developed with a pronounced {110} texture where the intensity of the texture increased with increasing vanadium content. Pronounced {110} textures have been observed when similar films were deposited at $U_B$ = -75 V [13]. In fact strong {110} textures are present in magnetron sputtered monolithically grown VN [14] films grown under similar bias voltage conditions indicating that under the deposition conditions used increasing the vanadium content favours the development of a {110} texture. This texture is in contrast to similar films which developed a pronounced {111} texture when deposited under similar conditions of bias voltage (i.e. $U_B$= -85V), but at a lower total pressure, P of $3.8x10^{-3}$ mbar T [13]. At the same bias voltage increasing the total gas pressure PT decreases the energy of the bombarding ions and therefore, has a similar influence on texture formation as reducing the bias voltage. Therefore, the texture developed at UBsy85 V using a total pressure $P_T$ = $5x10^{-3}$ mbar is similar to that developed at $U_B$ = -75V using a total pressure P = $3.8x10^{-3}$ mbar that is a T {110} texture in both cases.

*3.1.3. Residual stress hardness, sliding wear, coefficient of friction (μ) and adhesion*

Residual stress, hardness, sliding wear, coefficient of friction (m) and adhesion values for the four coatings under investigation are shown in Table 2. All the coatings investigated exhibited residual compressive stress states. The stresses varied between -5.2 GPa for sample 1 and -7.4 GPa for sample 3. The hardness values mirror those of the residual stresses with minimum and maximum

**Table 2** Texture coefficient T*, sliding wear, coefficient of friction, μ, hardness, adhesion and residual stress

| Sample | Texture coefficient, $T^*$ | | | Sliding wear ($m^3 N^{-11} m^{-11}$) | μ | Hardness Knoop $(Hk)_{0.25}$ | Adhesion critical load N ($L_c$) | Residual stress (GPa) |
|---|---|---|---|---|---|---|---|---|
| | (1 1 1) | (2 0 0) | (2 2 0) | | | | | |
| 1 | 0.2 | 1.7 | 4.1 | 4.5E−17 | 0.59 | 3377 | 55 | −5.2 |
| 2 | 0.3 | 1.1 | 4.3 | 2.8E−17 | 0.52 | 3378 | 42 | −6.4 |
| 3 | 0.3 | 0.9 | 4.9 | 5.8E−17 | 0.64 | 3752 | 55 | −7.4 |
| 4 | 0.3 | 0.9 | 4.5 | 1.76E−16 | 0.57 | 3451 | 49 | −6.6 |

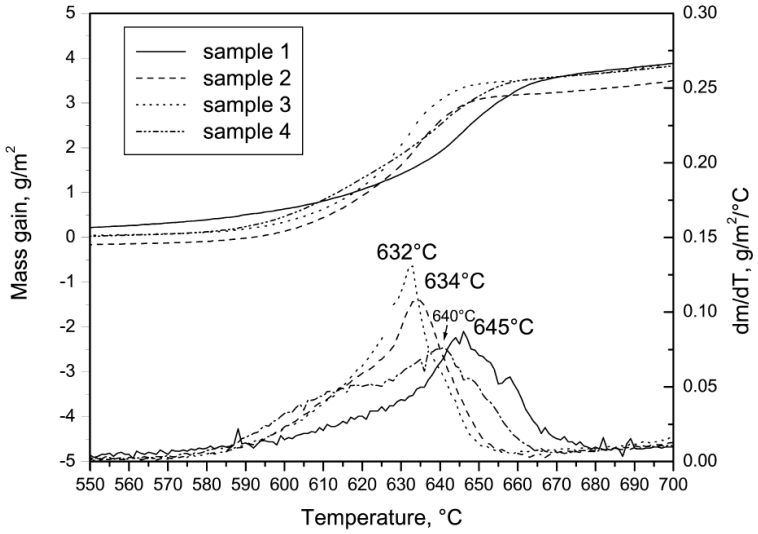


**Fig. 1.** Thermo-gravimetric oxidation measurement in air using a linear ramp of 1 °C $min^{-1}$ from 400 to 1000 °C for samples 1–4.

hardness values for samples 1 and 3, respectively. The sliding wear varied between 1.76 x $10^{-16}$ and 2.8 x $10^{-17}$ $m^3N^{-1}m^{-1}$, whilst the m varied between 0.52 and 0.64 with no clear trend of (Ti+Al):V ratio.

### *3.2. Oxidation studies*

*3.2.1. Thermal gravimetric analysis*

Fig. 1 plots thermal gravimetric analysis (TGA) oxidation rate measurements for TiAlN/VN coatings (coupons from samples 1 to 4) deposited on stainless steel substrates. The measurements were dynamic TGA using a linear temperature ramp (400–1000 °C at 1°C $min^{-1}$). The differentiated mass gains as a function of temperature are also displayed. Significant increases in mass gain (onset of rapid oxidation) occurred between 632 and 645 °C for all the coatings, which is in contrast to monolithic TiAlN coatings where the onset of rapid oxidation

occurred above 800 °C [15]. The temperature at which the onset of rapid oxidation occurred was also dependent on the (Ti+Al):V ratio in the coating, see Table 1. The higher the (Ti+Al):V ratio the higher the temperature at which rapid oxidation occurred, for example for sample 3 ((Ti+Al):V ratio 1.14) the onset of rapid oxidation was 632 °C whereas for sample 1 ((Ti+Al):V ratio 1.73) the onset of rapid oxidation was 645°C.


**Fig. 2.** A SEM of the surface of an oxidised TiAlN/VN coating sample 1, heat treated in air at 550 °C for 1 h.

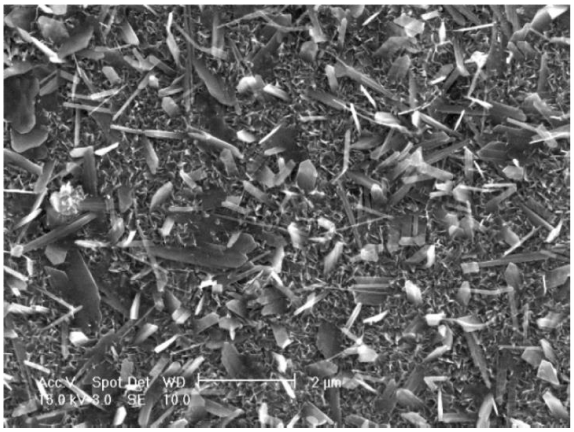


**Fig. 3.** A SEM of the surface of an oxidised TiAlN/VN coating sample 3, heat treated in air at 550 °C for 1 h.

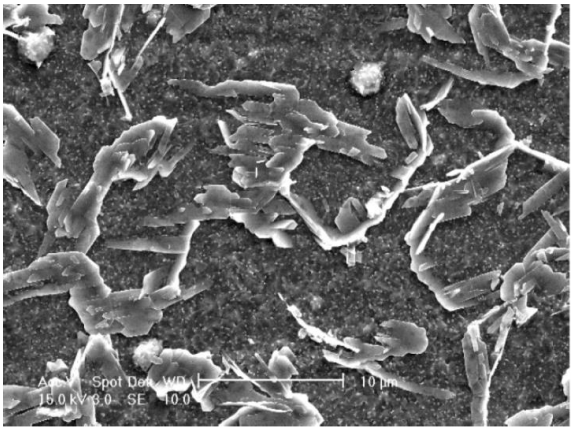


**Fig. 4.** A SEM of the surface of an oxidised TiAlN/VN coating, sample 1, heat treated in air at 600 °C for 1 h.

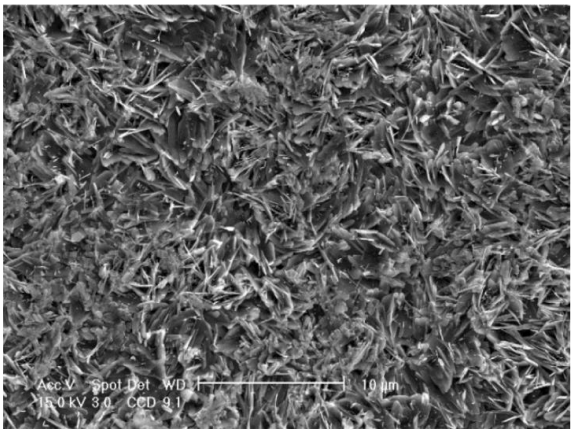


**Fig. 5.** A SEM of the surface of an oxidised TiAlN/VN coating, sample 3, heat treated in air at 600 °C for 1 h.

*3.2.2. Scanning electron microscopy*

Scanning electron micrographs (SEM) typical of the surfaces of samples 1–4 oxidised for 1 h in air at 550, 600, 640 and 670 °C are shown, respectively, in Figs. 2–8. After oxidation at 550 °C samples 1 and 4 exhibit an almost uniformly oxidised surface containing only a few needle-like particles, see Fig. 2. In contrast, samples 2 and 3 showed numerous needle-like particles at the surface, see Fig. 3. EDX analysis showed that the needle-like particles were rich in vanadium, i.e. $V_2O_5$. Increasing the heat treatment temperature to 600 °C resulted in the development of platelet type morphology at the surface in all four specimens. The volume

fraction of the platelets at the surface was the greatest in sample3 (compare Figs. 4 and 5), i.e. the coating containing the highest V content. EDX analysis showed the particles with platelet type morphology were richer in V than the surrounding regions thus leading one to the conclusion that they are $V_2O_5$. With the exception of sample 3 increasing the heat treatment temperature to 640 °C resulted in more extensive development of the plate-like morphology of the $V_2O_5$ phase, (compare Figs. 6 and 7). This supports the evidence from the XRD patterns which show increasing intensity of the

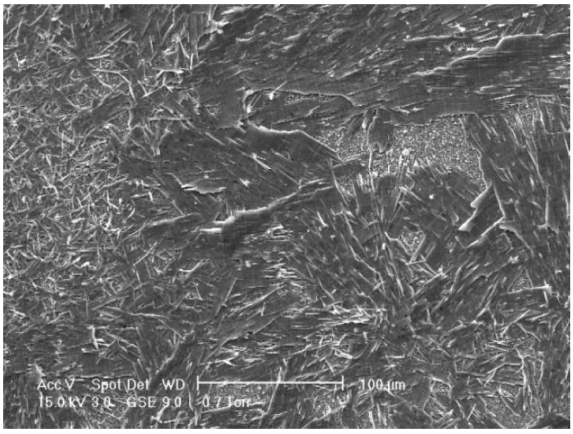


**Fig. 6.** A SEM of the surface of an oxidised TiAlN/VN coating, sample 1, heat treated in air at 640 °C for 1 h.

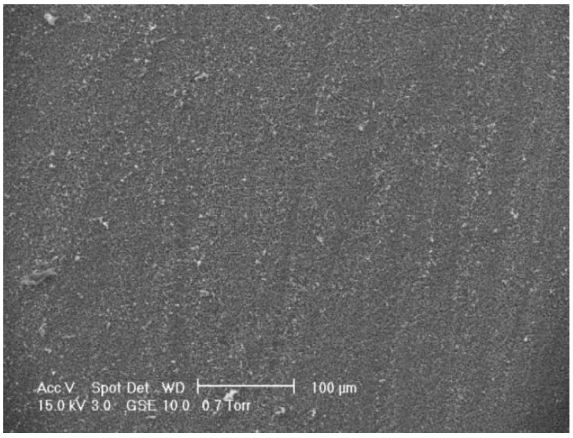


**Fig. 7.** A SEM of the surface of an oxidised TiAlN/VN coating, sample 3, heat treated in air at 640 °C for 1 h.

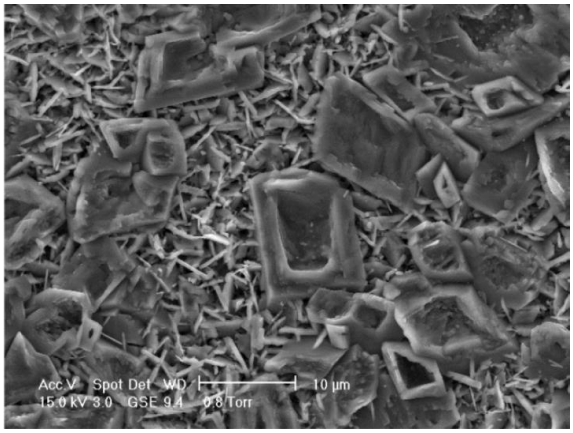


**Fig. 8.** A SEM of the surface of an oxidised TiAlN/VN coating, sample 1, heat treated in air at 670 °C for 1 h.

(001) texture of $V_2O_5$ for all coatings except sample 3 as the heat treatment temperature was increased to 640 °C. When the coatings were heat treated in air at 670 °C the plate like morphology completely disappeared to be replaced by regions with either blocky or needle like morphologies but there was no evidence of localised melting, see Fig. 8. EDX analysis showed the needle-like regions contained mainly Ti whilst the blocky regions contained both the elements Al and V.

*3.2.3. X-ray diffraction*

Glancing angle X-ray diffraction patterns (GAXRD, 1° incidence) of samples 1–4 heated in air at 550 °C are shown in Fig. 9. The following phases could be identified, $V_2O_5$ (41-

1426), $TiO_2$ (21-1276) and $AlVO_4$ (31-0034), together with the {1 1 1} and {200} (not shown in figure) reflections from the coating. However, when one compares the intensity of the (001) reflection for $V_2O_5$ in the GAXRD patterns it is clear that samples 1 and 4 contained relatively small amounts of $V_2O_5$ when compared with samples 2 and 3, the latter containing the highest intensity for the (001) reflection. The presence of coating peaks in the GAXRD pattern at 1° incidence clearly indicates an extremely thin oxide layer at the surface. A total oxide layer thickness of ~0.08 mm was calculated based on attenuation measurements of the {111} reflection from the coating. In

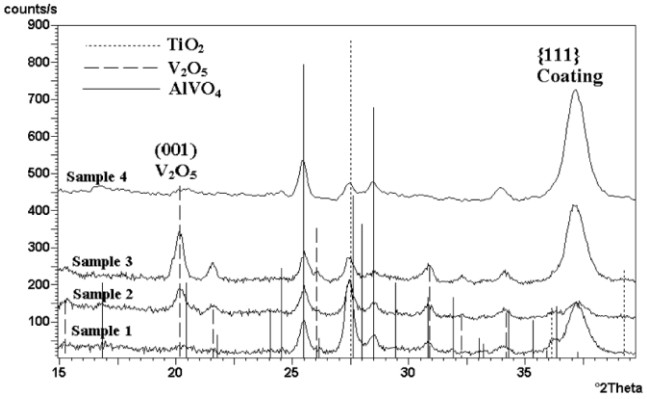


**Fig. 9.** GAXRD patterns of oxidised TiAlN/VN coating surfaces, heat treated in air at 550 °C for 1 h.

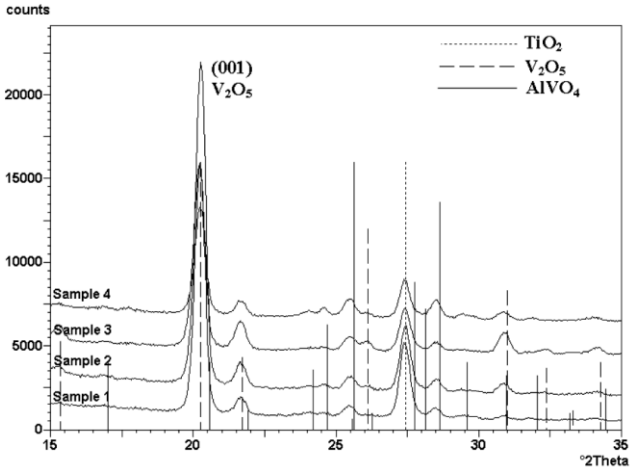


**Fig. 10.** θ/2θ XRD patterns of oxidised TiAlN/VN coating surfaces, heat treated in air at 600 °C for 1 h.

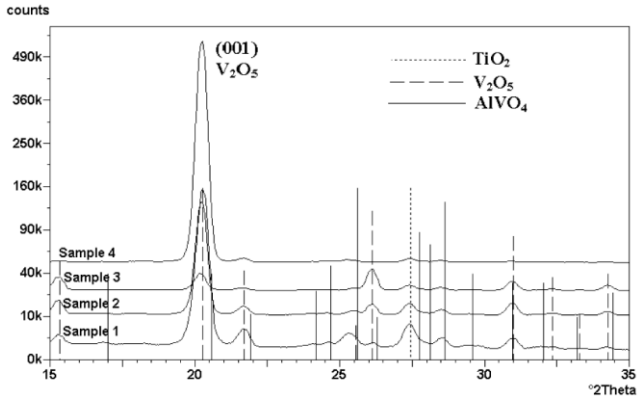


**Fig. 11.** θ/2θ XRD patterns of oxidised TiAlN/VN coating surfaces, heat treated in air at 640 °C for 1 h.

samples 1 and 4 where the Al:V ratio was almost unity the majority of any $V_2O_5$ formed was reduced to $AlVO_4$. In contrast, in samples 2 and 3 where the Al:V ratio was much less than

unity, more free $V_2O_5$ was present. XRD patterns ($\theta/2\theta$) of coatings heated in air for 1 h at 600 °C are shown in Fig. 10. In all cases the patterns contained the same phases as were present at 550 °C, i.e. $V_2O_5$, TiO2 and AlVO4. However, there was a dramatic increase in $V_2O_5$ relative to the other phases present. Furthermore, the $V_2O_5$ phase which formed was highly oriented with the majority of grain shaving their (001) planes parallel to the coating surface. The highly oriented (001) $V_2O_5$ phase identified in the $\theta/2\theta$ XRD patterns is consistent with the plate like morphology observed in the SEM images. However, there was still evidence of reflections from the coating (not shown in

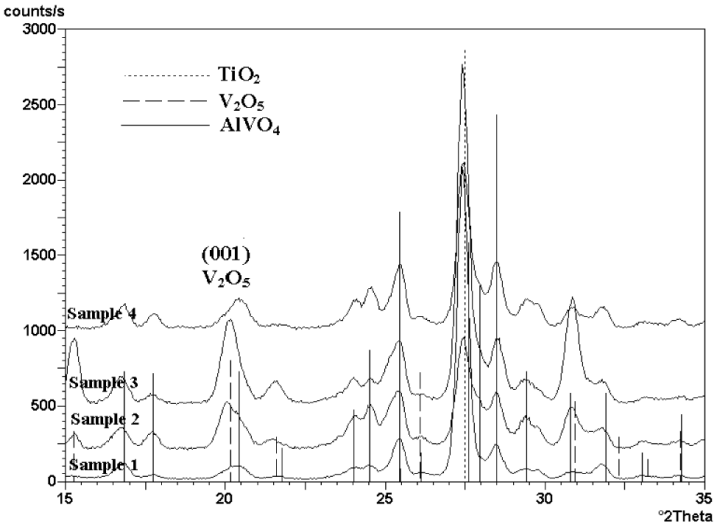


**Fig. 12.** $\theta/2\theta$ XRD patterns of oxidised TiAlN/VN coating surfaces, heat treated in air at 670 °C for 1 h.

figure) thus indicating that the coating was still intact. Increasing the heat treatment further toa temperature of 640 °C resulted, with the exception of sample 3, in further increases in the intensity of the (001) texture in the $V_2O_5$, Fig. 11 and is clearly consistent with the increased plate like morphology observed in the SEM images. flections from the coating have now disappeared indicating that the coating (not shown in figure) was almost completely oxidised.

Further increases in temperature to 670 °C, Fig. 12 resulted in a dramatic decrease in the intensity of the $V_2O_5$ and corresponding increase in the intensity of the $AlVO_4$. The strong (001) texture present in samples 1,2 and 4 after heat treating in air at 640 °C had completely disappeared. Thus, the $V_2O_5$ which had formed at the lower temperature was reduced by the formation of $AlVO_4$. This was clearly consistent with SEM observations which showed completely different surface morphologies after heating for 1 h in air at 670°C. Thus, the oxides present were mainly $TiO_2$ (rutile)and AlVO4 and indeed SEM and EDX analysis showed two phases one Ti rich and one Al and V rich.

$AlVO_4$ phase forms from a solid state reaction between $V_2O_5$ and $Al_2O_3$ of the following type [16–18].

$$V_2O_5 + Al_2O_3 = 2AlVO_4$$

However, according to Refs. [16–18] the reaction between $V_2O_5$ and $Al_2O_3$ to form $AlVO_4$ requires prolonged heating between 600 and 650 °C to go to completion. In the current work AlVO4 phase could be identified at temperatures as low as 550 °C, which is much lower than

previously observed. One possible explanation is that at 550 °C the reaction is occurring mainly at the surface where diffusion rates are at least an order of magnitude faster than in the bulk. It is well established that the onset of rapid oxidation of TiN to form rutile takes place at ;550 °C [19,20]. In TiAlN coatings the onset of rapid oxidation takes place above; 800 °C [15]. TiAlN oxidises to forma stable passive oxide double layer [19,20], the upper one Al rich and the lower one Ti rich which increases the oxidation resistance of TiAlN base coatings. Oxidation in TiAlN proceeds by the simultaneous diffusion of Al to the oxide/vapour interface and inward diffusion of O to the oxide/nitride interface. Thus, the oxidation resistance of TiAlN is conferred by the presence of a continuous $Al_2O_3$ rich layer at the surface. In TiAlN/VN coatings oxidised at 550 °C the presence of major reflections from the AlVO4 phase and only minor amounts of $V_2O_5$ (particularly in samples 1 and 4) would suggest that any $Al_2O_3$ which formed at the surface reacted with $V_2O_5$ to form $AlVO_4$. Therefore, the reaction of $Al_2O_3$ with $V_2O_5$ disrupts the protective $Al_2O_3$ layer from TiAlN/VN coatings. In the absence of a protective $Al_2O_3$ layer increasing the oxidation temperature to 600 or 640 °C results in rapid oxidation of the TiAlN/VN coatings (Fig. 1) to produce $V_2O_5$, TiO2 and possibly $Al_2O_3$ although no crystalline phase of $Al_2O_3$ has been identified. No further significant increases in $AlVO_4$ were observed indicating little or no further reaction between $V_2O_5$ and $Al_2O_3$ in the bulk at these temperatures. This is consistent with the SEM images which show penetration of the surface by platelets of $V_2O_5$ at 600 and 640 °C, see Figs. 4–6. Increasing the temperature to 670 °C results in the formation of AlVO4 that was clearly identified by both XRD and EDX analysis. Therefore, at 670 °C the temperature is sufficiently high for the reaction of $V_2O_5$ with $Al_2O_3$ to proceed in the bulk to form $AlVO_4$ [16–18]. The formation of $V_2O_5$ is believed to be critical to the low friction behaviour of these coatings. At 550 °C the oxidation of V appears to be dominated by the formation of $AlVO_4$. Only at temperatures of 600 and 640 °C significant quantities of $V_2O_5$ are formed leading one to the conclusion that these temperatures must be generated locally before low friction conditions prevail.

## 4. Conclusions

1) The onset of rapid oxidation in these coatings takes place at temperatures between 632 and 645 °C, which is ~150 °C lower than for monolithic TiAlN coatings. The higher the (Ti+Al):V ratio the higher the temperature of onset of rapid oxidation.
2) A reaction which occurs between $Al_2O_3$ and $V_2O_5$ to form $AlVO_4$ was responsible for disrupting the formation of $Al_2O_3$ which imparts oxidation resistance on TiAlN based coatings. This reaction lowers the oxidation resistance of TiAlN/VN nano-scale multilayer coatings when compared with monolithic TiAlN based coatings.
3) The relative amounts of $V_2O_5$ which formed was observed to depend on the (Ti+Al):V ratio.
4) The $V_2O_5$ phase with a plate like morphology was oriented with the (001) plane parallel to the coating surface.

## Acknowledgments

Financial support from Engineering and Physical Science Research Council (EPSRC), UK, Grant No GR/N23998y01 is acknowledged.

## References

[1] W.-D. Munz, D.B. Lewis, P.Eh. Hovsepian, C. Schonjahn, A.Ehiasarian, I.J. Smith, Surf. Eng. 17 (2001) 15.

[2] D.B. Lewis, I. Wadsworth, W.-D. Munz, R. Kuzel Jr., V. Valvoda, Surf. Coat. Technol. 116–119 (1999) 284.

[3] I. Wadsworth, I.J. Smith, L.A. Donohue, W.-D. Munz, Surf. Coat. Technol. 94–5 (1997) 315.

[4] P.Eh. Hovsepian, D.B. Lewis, W.-D. Munz, S.B. Lyon, M. Tomlinson, Surf. Coat. Technol. 120–121 (1999) 535.

[5] P.Eh. Hovsepian, D.B. Lewis, W.-D. Munz, Surf. Coat. Technol.133–134 (2000) 166.

[6] W.-D. Munz, D. Schulze, F. Hauzer, Surf. Coat. Technol. 50 (1992) 169.

[7] L.A. Donohue, W.-D. Munz, D.B. Lewis, et al., Surf. Coat. Technol. 93 (1997) 69.

[8] P.Eh. Hovsepian, D.B. Lewis, W.-D. Munz, A. Rouzaud, P. Juliet, Surf. Coat. Technol. 116–119 (1999) 727.

[9] D.B. Lewis, I.P. Wadsworth, W.-D. Munz, R. Kuzel Jr., V. Valvoda, Surf. Coat. Technol. 116–119 (1999) 284.

[10] P.Eh. Hovesepian, D.B. Lewis, W.-D. Munz, Surf. Coat. Technol.133–134 (2000) 166.

[11] G.B. Harris, Phil. Mag. 43 (1952) 113.

[12] D.E. Geist, A.J. Perry, J.R. Treglio, V. Valvoda, D. Rafaja, Adv. X-ray Anal. 38 (1995) 471.

[13] D.B. Lewis, P. Eh. Hovsepian, W.-D. Munz, Seventh International Symposium on Trends and Applications of Thin Films, TAFT 2000 Nancy France, 28–30 March 2000, Socie´te´ Francaisedu Vide.

[14] G. Farges, E. Beuprez, M.C. Staine-Catherine, Surf. Coat. Technol. 54–55 (1992) 115.

[15] W.-D. Munz, J. Vac. Sci. Technol. A 4 (1986) 2717.

[16] O. Yamaguchi, T. Uegaki, Y. Miyata, K. Shimizu, J. Am. Ceram. Soc. 70 (8) (1987) 198.

[17] F.H.A. Abdalla, G.A. El-Shobaky, N.A. Hassan, Bull. Soc. Chim. Belg. 103 (11) (1994) 665.

[18] 2000 JCPDS—International Centre for Diffraction Data.

[19] D. McIntyre, J.E. Greene, G. Ha˚kansson, J.-E. Sundgren, W.-D. Munz, J. Appl. Phys. 67 (1990) 1542.

[20] L.A. Donohue, I.J. Smith, W.-.D. Munz, I. Petrov, J.E. Greene, Surf. Coat. Technol. 94y95 (1997) 226.